

Dynamic hydration valve controlled ion permeability and stability of NaK channel

Rong Shen^{1,*}, Wanlin Guo^{1,*} & Wenyu Zhong¹

¹*Institute of Nano Science, Nanjing University of Aeronautics and Astronautics, Nanjing 210016, China*

**These authors contributed equally to this work*

The K^+ , Na^+ , Ca^{2+} channels are essential to neural signalling, but our current knowledge at atomic level is mainly limited to that of K^+ channels. Unlike a K^+ channel having four equivalent K^+ -binding sites in its selectivity filter¹⁻³, a NaK channel conducting both Na^+ and K^+ ions has a vestibule in the middle part of its selectivity filter, in which ions can diffuse but not bind specifically^{4,5}. However, how the NaK channel conducts ions remains elusive. Here we find four water grottos connecting with the vestibule of the NaK selectivity filter. Molecular dynamics and free energy calculations show that water molecules moving in the vestibule-grotto complex hydrate and stabilize ions in the filter and serve as a valve in conveying ions through the vestibule for controllable ion permeating. During ion conducting, the water molecules are confined within the valve to guarantee structure stability. The efficient exquisite hydration valve should exist and play similar roles in the large family of cyclic nucleotide-gated channels which have similar selectivity filter sequences. The exquisite hydration valve mechanism may shed new light on the importance of water in neural signalling.

Fifty five years ago, Hodgkin and Huxley found that Na^+ and K^+ permeability through cell membranes is the root of neuron signalling⁶. In the following decades our basic understanding of ion channels has been enriched by extensive electrophysiological researches, especially with the aid of patch-clamp techniques, but it is the finding of K^+ channel KcsA crystal structure shows us the first time the atomic mechanism of how ions are selected and permeated in an ion channel. K^+ channel has a selectivity filter sequence of TVGYG and forms a simple one-dimensional pore, which consists of four equivalent K^+ -binding sites numbered 1~4 from the extracellular to the intracellular sides, for selectively conducting K^+ ions¹⁻³. The ions binding in the selectivity filter are necessary for channel stability and a water molecule must take the site between two succeeding ions and conduct through the channel with the ions^{7,8}.

The newly found NaK channel conducting both K^+ and Na^+ ions^{4,9} has a filter sequence of ₆₃TVGDG₆₇, different from that of a potassium channel but similar to the specific sequence TIGET of most cyclic nucleotide-gated (CNG) channels which work in our photoreceptors and olfactory cells^{10,11}. The structure of the NaK channel should have great potential to unveil the secret of permeation of ions other than K^+ . However, the NaK crystal structure was obtained in a Ca^{2+} rich NaCl or KCl solution with a Ca^{2+} blocking at the mouth of the extracellular entryway and two ions binding adjacently at two cation binding sites equivalent to sites 3 and 4 of a K^+ channel. The region corresponding to sites 1 and 2 of a K^+ channel becomes a vestibule near residues GD⁴ (Fig. 1a), in which no ion can binding specifically as shown by the experiment. Therefore, how the NaK channel can maintain its stability without of the blocking Ca^{2+} , and how ions can conduct through the

channel weakened by the vestibule become very important to understand ion permeating mechanism other than K^+ channels. Here we find four water grottos connecting with the vestibule in the structure of the NaK channel, and they form a vestibule-grotto (V-G) complex in a plane perpendicular to the ion conducting pore. Each grotto is formed between two adjacent filter loops at Gly65-Asp66 and the p-loop helices at Tyr55-Thr60. The overall profile of the V-G complex is shown in Fig. 1b, c, which was obtained by probing the protein structure (PDB ID 2AHZ) with the program HOLE¹².

As no specific ion binding site in the vestibule, how ions line in the NaK selectivity filter remains elusive. We conduct extensive all-atom molecular dynamics (MD) simulations (see section Methods and Supplementary Fig. S2) with all possible initial permutation and combination of Na^+ and K^+ ions and water molecules lining in the NaK selectivity filter (Supplementary Tables S1 and S2). The resulted stable ion binding configurations are simple and uniform for pure K^+ or Na^+ lining and mixed K^+ and Na^+ linings (Fig. 2a-d): two ions near sites 1 and 3 with one water molecule between them in the vestibule. For convenience, we number all the possible sites by the equivalent sites of a K^+ channel (Fig. 2). Additionally, site “01” between sites 0 and 1 among the four Asp66 backbone carbonyl oxygen atoms, and site “23” between sites 2 and 3 among the four Val64 carbonyl oxygen atoms are assigned here. Not like the experimental results with a Ca^{2+} ion blocking at site ext, a K^+ ion can specifically bind at site 1 or a Na^+ ion at site 01 in the vestibule, and it is always partially hydrated by the water molecule in the vestibule. K^+ can set exactly at site 3, while the smaller Na^+ ion tends to take a higher position at site 23. When a K^+ ion sets at site 1, no specific water molecule at site 0, may due to the lower

position of the K^+ ion and its weaker interaction with the water molecule. However, when a Na^+ ion sets at site 01, one water molecule always sets stably at site 0 with its oxygen atom facing the ion. When both sites 01 and 23 are taken by Na^+ ions, two water molecules can enter the vestibule between them frequently. In all the relaxed cases, no specific water or ion can bind stably at site 4. Loss of ion in site 1 or 3 will lead to instability of the filter, and lack of water molecule in the vestibule is also an instable state as water has to be supplied from the extracellular water pits above the grottos around the extracellular entrance (Supplementary Fig. S3). It is also important to note that without of Ca^{2+} blocking, the vestibule is remarkably narrower than in the reported Ca^{2+} blocked crystal structure due to the attraction of the cation near site 1 (Supplementary Fig. S4a), leading to a thin neck between the vestibule and grotto, as shown by the red belts (Fig. 2e), which provides high energy barrier to confine the water molecules in the vestibule and grottos in a mostly lentic or inactive state.

Without pulling force on the ions in the selectivity filter, no ion permeation can occur in the MD simulations. To peer into the ion permeation mechanism, we applied force or bias voltage on each ion along the filter pore upward and perform the so called steered MD (SMD) simulations. Here we concentrated on the situation of pure K^+ ions and water molecules lining in the NaK filter to show the permeating mechanism. Simulations for 3 K^+ ions (at sites 01, 3 and 4) subjected to force of 80, 120, 160 and 200 pN/ion are performed, with or without of a fourth free or forced K^+ ion in the cavity being considered (see Supplementary Information). It is shown that only when the fourth ion in the cavity is considered and the force on each ion in the filter is up to 160 pN/ion (equivalent to a

membrane voltage bias about 1V/nm), ion conduction can occur in several nanoseconds. In a previous MD study of the NaK channel, Vora et al.¹³ also reported that a membrane potential of 1.2 V/nm or 1.4 V/nm could result in an outward K⁺ conduction rate of 0.3 or 0.4 ions per ns, respectively, and the average number of ions in the selectivity filter region was 3.5-4 ions.

With 160 pN or a membrane voltage bias about 1V/nm upward on each of the three ions and one water molecule in each grotto initially, the configuration of the selectivity filter approaches to that of the crystal structure (Supplementary Fig. S4b), and the water molecules in the V-G complex become highly activated (Supplementary Fig. S5). Comparing with the relaxed state, an extracellular water molecule comes to bind at site 0 and the ion in the cavity goes up into site 4 stably. Although no permeation occurs with the 3 forced ions, the 5 water molecules in the V-G complex can flow easily between the vestibule and grottos (Supplementary Fig. S5b). When another water molecule comes into the vestibule from one of the grottos, one of the two water molecules in the vestibule will leave the vestibule to a grotto succeedingly. This is also observed in SMD simulation with a biologically realistic electric field of 0.05 V/nm being applied to the selectivity filter. It is interesting that the free energy barrier for a water molecule moving from the vestibule into the grotto can be significantly reduced if there are two water molecules in the vestibule (Fig. 3d). Therefore, water molecules in the grottos are necessary for water movement in the V-G complex. When a 4th K⁺ ion bearing the same 160 pN force or 1V/nm bias voltage upward is added in the cavity at 7 ns in the SMD simulation (simulation CIII, see Supplementary Table S3), ion flowing is ignited (Fig. 3a). The coupling movement of ions

and water in the filter and the V-G complex can be featured by snapshots shown in Supplementary Fig. S6.

In real biologic situations, ion permeating rate is exceedingly slower even than all the SMD simulations we can handle by the present technology. Guided by the SMD simulations, we further perform careful equilibrium free energy profile or potential of mean force (PMF) analyses, which governs the concerted transition of ions along the pore^{14, 15}. The one-dimensional PMF $W(Z_{\text{ion}2})$ for ion-2 moving from site 3 to site 2, and two-dimensional PMF $W(Z_{\text{ion}1}, Z_{\text{ion}2})$ for ion-1 moving out and ion-2 moving up to site 1 are calculated with umbrella sampling simulations¹⁶ and shown in Fig. 3b and c, respectively. It is found that with one water molecule in each grotto, the energy barrier for the transition of ion-2 from site 3 to site 2 can be reduced by about 3 kcal mol⁻¹ (Fig. 3b). Analysis of the sampling trajectories reveals that one water molecule in the grottos indeed enters into the vestibule to hydrate and stabilize ion-2. This is consistent with the SMD simulations. Figure 3c reveals two possible pathways for the concerted translocation of ion-1 and ion-2 while ion-3 and ion-4 are constrained tightly at site 3 and site 4, respectively. Both pathways have the highest free energy barriers about 4 kcal mol⁻¹. Pathway (a) is coincident well with the SMD trajectory (ion-1 jumps out firstly, then ion-2 moves up to site 1) (Fig. 3a). Along pathway (b), ion-1 and ion-2 move simultaneously, but ion-2 moves faster than ion-1 and pushes ion-1 to exit from the filter. Further analysis indicates that the existence of pathway (b) is mainly contributed to the lateral displacement of ion-2 in the wide vestibule.

Summarily, the molecular dynamics simulations and the energy profile analyses show highly coincident results, and we are able to scheme the ion conducting mechanism of the NaK channel in Fig. 4 with K^+ ions as example. In the closed state, three ions locate in the channel, binding at sites 1, 3 and in the cavity, respectively, and no water molecule sets at site 0 (Fig. 4a). Water molecules in the V-G complex are confined in a lentic state (Fig. 4h) initially. When the channel is opened, the ion in the cavity will go up into site 4 with the ions in sites 1 and 3 moving up a bit (Fig. 4b). This induces an extracellular water molecule to come into and bind at site 0 to coordinate the raised ion in site 1 (Fig. 4c). A further K^+ ion entering from the cytoplasm to the cavity and a water molecule entering the vestibule from one grotto will ignite the ion flowing (Fig. 4d, e). Noskov and Roux⁹, Vora et al.¹³, and Shen and Guo (unpublished results) also showed that the average hydration number of K^+ is up to 2~3 at site 2 in the vestibule, obviously higher than that at the site 2 in the KcsA selectivity filter (1.4 ± 0.1). Initially, the ion in site 3 hops up to the vestibule, then the ion at site 4 hops to site 3 and the ion in the cavity enters site 4 succeedingly (Fig. 4f). After this preparation, the top ion has gathered enough energy to jump out and the ion in the vestibule will move up to site 1 with the two hydrating water molecules jinking apart (Fig. 4g). Finally, one of the two hydrating water molecules returns into one grotto, completing one permeation cycle. The water molecules in the V-G complex are in an active state during the whole permeation cycle (Fig. 4i-k). Not like in a K^+ channel, water molecules do not flow through the selectivity filter with the conducting ions but are confined within the valve in the NaK channel so that the limited ion binding sites can always be taken by ions to maintain the filter in stable. The existence of the grottos and their simple and beautiful

structure-function correlation can be expected in the whole family of CNG channels which have similar selectivity filter sequences.

Methods

Whole atomic model of the NaK channel in membrane. The basic MD model (see Supplementary Fig. S2) consists of the 2.8 Å resolution structure (PDB ID 2AHZ) of NaK in its K⁺-bound state⁴, embedded in a fully hydrated dimyristoylphosphatidylcholine (DMPC) lipid bilayer surrounded by a 200 mM KCl aqueous salt solution box. It contains totally 42,871 atoms, including 6,900 protein atoms, 127 DMPC lipid molecules (67 and 60 in the extracellular and intracellular sides, respectively) with 14,986 atoms, 20,955 water atoms, 3 K⁺ in the pore, and 6 K⁺ and 21 Cl⁻ ions in the bulk solution. The cavity is filled with 38 water molecules initially. Ionizable residues are set to their default protonation state. The whole system is in an electro-neutral state.

Molecular Dynamics Simulations. All MD simulations were performed using the program NAMD¹⁷. The CHARMM27 force field was used for protein and phospholipids¹⁸. The TIP3P model was used for water¹⁹. The Lennard-Jones parameters for K⁺ and Na⁺ ions were modified following the previous results in ref. (20). Periodic boundary conditions were applied in all directions. Electrostatic forces were calculated without cutoff, using the particle mesh Ewald (PME) method²¹ with a grid density of at least 1 Å⁻³. Smooth (8-10 Å) switching off was applied for the van der Waals interactions. All simulations were carried out with a time step of 1 fs. The Langevin dynamics was employed to control the

temperature at constant 310 K, and the Nosé-Hoover Langevin piston method^{22, 23} was used to maintain the pressure at 1 atm. Additional details on simulation procedures are given in Supplementary Information.

Free energy calculations. The equilibrium free energy profiles for ion conducting through the selectivity filter and water molecule moving between the vestibule and grotto are calculated with umbrella sampling¹⁶ and the adaptive biasing force (ABF)²⁴ methods as described in detail in Supplementary Information.

1. Doyle, D. A. *et al.* The structure of the potassium channel: molecular basis of K⁺ conduction and selectivity. *Science* **280**, 69-77 (1998).
2. Morais-Cabral, J. H., Zhou, Y. & MacKinnon, R. Energetic optimization of ion conduction rate by the K⁺ selectivity filter. *Nature* **414**, 37-42 (2001).
3. Zhou, Y., Morais-Cabral, J. H., Kaufman, A. & MacKinnon, R. Chemistry of ion coordination and hydration revealed by a K⁺ channel-Fab complex at 2.0 Å resolution. *Nature* **414**, 43-48 (2001).
4. Shi, N., Ye, S., Alam, A., Chen, L. & Jiang, Y. Atomic structure of a Na⁺- and K⁺-conducting channel. *Nature* **440**, 570-574 (2006).
5. Alam, A., Shi, N. & Jiang, Y. Structural insight into Ca²⁺ specificity in tetrameric cation channels. *Proc. Natl. Acad. Sci. USA* **104**, 15334-15339 (2007).
6. Hodgkin, A. L. & Huxley, A. F. A quantitative description of membrane current and its application to conduction and excitation in nerve. *J. Physiol. (Lond)* **117**, 500-544 (1952).

7. Aqvist, J. & Luzhkov, V. Ion permeation mechanism of the potassium channel. *Nature* **404**, 881-884 (2000).
8. Zhou, M. & MacKinnon, R. A mutant KcsA K⁺ channel with altered conduction properties and selectivity filter ion distribution. *J. Mol. Biol.* **338**, 839-846 (2004).
9. Noskov, S. Y. & Roux, B. Importance of hydration and dynamics on the selectivity of the KcsA and NaK channels. *J. Gen. Physiol.* **129**, 135-143 (2007).
10. Kaupp, U. B. & Seifert, R. Cyclic nucleotide-gated ion channels. *Physiol. Rev.* **82**, 769-824 (2002).
11. Matulef, K. & Zagotta, W. N. Cyclic nucleotide-gated ion channels. *Annu. Rev. Cell Dev. Biol.* **19**, 23-44 (2003).
12. Smart, O. S., Goodfellow, J. M. & Wallace, B. A. The pore dimensions of gramicidin A. *Biophys. J.* **65**, 2455-2460 (1993).
13. Vora, T., Bisset, D. & Chung, S. H. Conduction of Na⁺ and K⁺ through the NaK channel: Molecular and Brownian dynamics studies. *Biophys. J.* In press.
14. Berneche, S. & Roux, B. Energetics of ion conduction through the K⁺ channel. *Nature* **414**, 73-77 (2001).
15. Roux, B. Statistical mechanical equilibrium theory of selective ion channels. *Biophys. J.* **77**, 139-153 (1999).
16. Torrie, G. M. & Valleau, J. P. Nonphysical sampling distributions in Monte Carlo free-energy estimation: umbrella sampling. *J. Comput. Phys.* **23**, 187-199 (1977).

17. Phillips, J. C. *et al.* Scalable molecular dynamics with NAMD. *J. Comput. Chem.* **26**, 1781-1802 (2005).
18. MacKerell, A. D. Jr. *et al.* All-atom empirical potential for molecular modeling and dynamics studies of proteins. *J. Phys. Chem. B* **102**, 3586-3616 (1998).
19. Jorgensen, W. L., Chandrasekhar, J., Madura, J. D., Impey, R. W. & Klein, M. L. Comparison of simple potential functions for simulating liquid water. *J. Chem. Phys.* **79**, 926-935 (1983).
20. Roux, B. & Berneche, S. On the potential functions used in molecular dynamics simulations of ion channels. *Biophys. J.* **82**, 1681-1684 (2002).
21. Essmann, U. *et al.* A smooth particle mesh Ewald method. *J. Chem. Phys.* **103**, 8577-8593 (1995).
22. Feller, S. E., Zhang, Y. H., Pastor, R. W. & Brooks, B. R. Constant pressure molecular dynamics simulation: The Langevin piston method. *J. Chem. Phys.* **103**, 4613-4621 (1995).
23. Martyna, G. J., Tobias, D. J. & Klein, M. L. Constant pressure molecular dynamics algorithms. *J. Chem. Phys.* **101**, 4177-4189 (1994).
24. Henin, J. & Chipot, C. Overcoming free energy barriers using unconstrained molecular dynamics simulations. *J. Chem. Phys.* **121**, 2904-2914 (2004).
25. Humphrey, W., Dalke, A. & Schulten, K. Vmd: visual molecular dynamics. *J. Mol. Graph.* **14**, 33-38 (1996).

Supplementary Information is linked to the online version of the paper at www.nature.com/nature. A figure summarizing the main result of this paper is available in Supplementary Information.

Acknowledgments We thank Youxing Jiang for providing us important details of their experiments and Changfeng Chen for helpful discussions. The work is supported by 973 Program (2007CB936204), the Ministry of Education (No. 705021, IRT0534) and National NSF (10732040) of China.

Author Contributions W.G. and R.S. contributed to design, modelling and mechanism analyses. W.Z. mainly contributed to the modelling methods and some discussions.

Author Information Reprints and permissions information is available at <http://npg.nature.com/reprintsandpermissions>. Correspondence and requests for materials should be addressed to W.G. (wlguo@nuaa.edu.cn).

Figure Legends

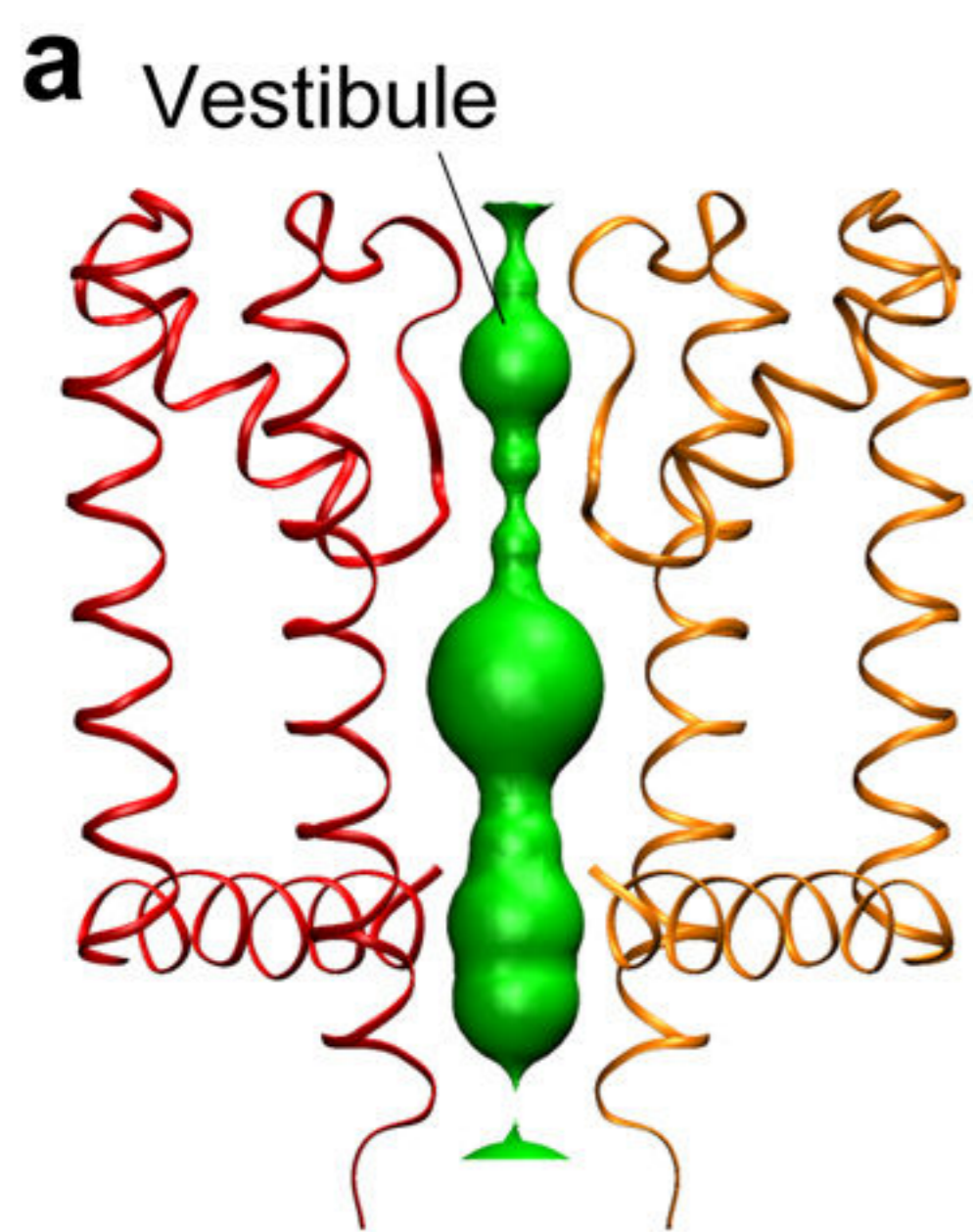
Figure 1 The structure feature of the NaK channel. **a**, The central pore. **b**, Side view of two grottos from the pore. **c**, Top view of the vestibule-grotto complex. The red belts between the grottos and vestibule show the narrow necks with radius $<1.15 \text{ \AA}$. For clearance, only two monomer subunits are shown in (**a**, **b**). Figures 1, 2 were generated with the programs HOLE¹² and VMD²⁵.

Figure 2 Ions binding in the pore and water molecules in the grottos. The stable configurations in the relaxed states for **a**, pure K^+ ions; **b**, pure Na^+ ions; **c** and **d**, mixed K^+ and Na^+ ions in the filter. **e**, The corresponding water movement confined in the vestibule-grottos where the oxygen atom of water is in specific colored ball and hydrogen atom in smaller white ball. The rest water molecules are in inked-sticks, K^+ and Na^+ ions are represented in yellow and ice-blue spheres, respectively. In **a-d** the front and rear subunits are removed for clarity.

Figure 3 Movement and free energy profiles of ions and water molecules in the filter pore and the vestibule-grotto complex during ion conducting. **a**, Ions conducting in the filter. Red lines are the tracks of the oxygen atoms of the filter, blue curves are ions tracks and green shows the tracks of water molecules in the vestibule. The ions are numbered ion-1 to ion-4 from the extracellular to the intracellular sides. **b**, The one-dimensional PMF $W(Z_{\text{ion}2})$ for the transition of ion-2 from S3 to S2 with or without one water molecule in each grotto while the three other ions are constrained tightly at different positions along the pore ($Z_{\text{ion}1} : 13.5 \text{ \AA}$, $Z_{\text{ion}3} :$

2.0 Å and $Z_{\text{ion4}} : -2.0 \text{ Å}$, respectively, according to the SMD simulation trajectory). **c**, The two-dimensional PMF $W(Z_{\text{ion1}}, Z_{\text{ion2}})$ as a function of positions of ion-1 and ion-2 while ion-3 and ion-4 are constrained tightly at 5.5 Å and 1.5 Å, respectively. Contours are drawn at every 1 kcal mol⁻¹. Two pathways are highlighted: a (thick dashed line) and b (thin dashed line). **d**, The free energy to move a water molecule from the vestibule to grotto with or without of a succeeding water molecule to the vestibule from another grotto.

Figure 4 Schematic representation of the K⁺ ion permeation controlled by the dynamic hydration valve formed in the vestibule-grotto complex. Ion conducting is ignited when the vestibule is in green, and ion conducting is ceased when the vestibule is in red.



Extracellular

Selectivity
filter

Cavity

Entryway

Intracellular

